SAND2014-15888C

Available online at www.sciencedirect.com

ScienceDirect

Energy Procedia 00 (2015) 000–000

Energy Procedia

www.elsevier.com/locate/procedia

International Conference on Concentrating Solar Power and Chemical Energy Systems, SolarPACES 2014

Metallic phase change material thermal storage for dish Stirling

C.E. Andraka[a*], A.M. Kruizenga[b], B.A. Hernandez-Sanchez[c], E.N. Coker[c]

[a] *Sandia National Laboratories, CSP Department, PO 5800 MS 1127, Albuquerque NM 87185-1127*
[b] *Sandia National Laboratories, PO 969 MS 9403, Livermore CA 94551*
[c] *Sandia National Laboratories, Advanced Materials Laboratory PO 5800 MS 1349, Albuquerque NM 87185-1349*

Abstract

Dish-Stirling systems provide high-efficiency solar-only electrical generation and currently hold the world record at 31.25%. This high efficiency results in a system with a high possibility of meeting the DOE SunShot goal of $0.06/kWh. However, current dish-Stirling systems do not incorporate thermal storage. For the next generation of non-intermittent and cost-competitive solar power plants, we propose adding a thermal energy storage system that combines latent (phase-change) energy transport and latent energy storage in order to match the isothermal input requirements of Stirling engines while also maximizing the exergetic efficiency of the entire system.

This paper reports current findings in the area of selection, synthesis and evaluation of a suitable high performance metallic phase change material (PCM) as well as potential interactions with containment alloy materials. The metallic PCM's, while more expensive than salts, have been identified as having substantial performance advantages primarily due to high thermal conductivity, leading to high exergetic efficiency. Systems modeling has indicated, based on high dish Stirling system performance, an allowable cost of the PCM storage system that is substantially higher than SunShot goals for storage cost on tower systems. Several PCM's are identified with suitable melting temperature, cost, and performance.

Peer review by the scientific conference committee of SolarPACES 2014 under responsibility of PSE AG.

Keywords: CSP; Dish Stirling; Phase change storage; Heat pipe; Concentrating Solar Power;

* Corresponding author. Tel.: +1-505-844-8573; fax: +1-505-845-3366.
E-mail address: ceandra@sandia.gov

Peer review by the scientific conference committee of SolarPACES 2014 under responsibility of PSE AG.

1. Background

Previous efforts by our team have determined that coupling thermal storage with dish Stirling systems has a high potential of success, and results in a net financial benefit if the cost of storage is below \$82/kWh$_{th}$ (LCOE) or \$99/kWh$_{th}$ (profit)[1, 2]. Development of a storage option for dish Stirling requires identification or development of the storage system configuration, understanding the heat transfer fluids and techniques, and characterization of the storage media. Our prior work has identified the optimal solar multiple at 1.25 (94kW$_{th}$ input) and 6 hours of storage based on southern California weather patterns and rate structures.

For the next generation of non-intermittent and cost-competitive solar power plants, we proposed a thermal energy storage system that combines latent-energy transport and latent-energy storage in order to maximize the exergetic efficiency of the entire system and matches the isothermal input feature of the Stirling cycle engine. A configuration that allows implementation on the movable portion of the dish—eliminating the need for high-temperature rotating or flexible joints and minimizing heat losses in thermal transport is also needed. The system would use Sandia-developed high-performance sodium heat pipes to facilitate extension of storage to large (25 kWe) systems. This configuration was originally proposed as an ARPAe HEATS project [3] and detailed in a report [1].

Our proposed configuration centers on providing transport that enables storage and engine mounting on the rear of the dish rather than at the focus. This allows a substantially higher thermal storage mass than can be supported on the power conversion unit (PCU) cantilever boom, facilitating storage durations of six or more hours. Figure 1 schematically shows the proposed system layout (not to scale). The dish is typically 11-12m in diameter for 25kW$_e$, and the storage media is approximately 1m^3. The storage unit, in total, may weigh about 5000kg, while the rotating mass of a near-commercial dish weighs about 7000kg. A pumped condensate sodium heat pipe transports energy from the solar receiver to the storage media nearly isothermally. The storage media proposed is a metallic Phase Change Material (PCM), selected for high-density isothermal storage. A second isothermal heat pipe transports the thermal energy from storage to the engine, providing high flux to the engine through condensation. The separate heat pipe systems provide a "thermal diode" effect to reduce thermal losses when operating from stored energy.

The proposed approach leverages the existing high-temperature (700–800°C), high efficiency dish Stirling system, and provides a storage option. The simplicity of this design contrasts trough and tower high-temperature storage systems which need further development to provide a high-temperature thermodynamic cycle and receiver, as well as high-concentration optics suitable to limit collection losses.

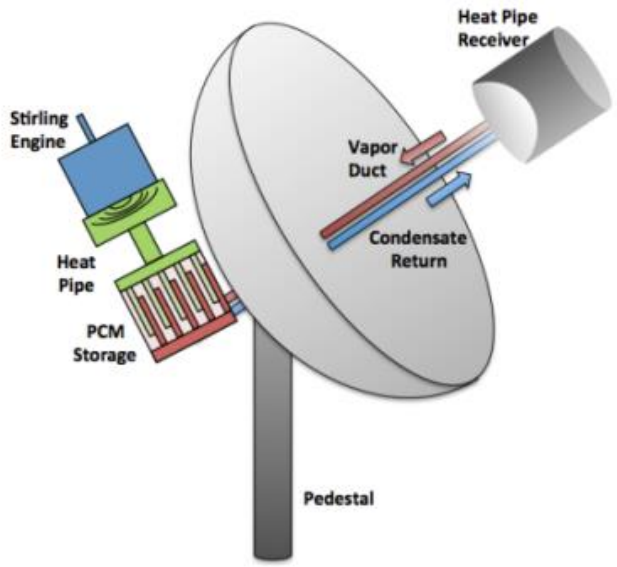

Figure 1. Schematic layout (not to scale) of proposed latent energy storage system for dish Stirling power generation.

The phase change material, due to high thermal throughput, must be a metallic storage media in order to achieve a goal of 95% exergy efficiency [2, 4]. The metallic-based options provide sufficient thermal conductivity that can reduce the number of heat pipe tubes used by about an order of magnitude compared to salt PCM options. The metallic PCM should ideally melt at 750-800°C to match the high performance Stirling engines available. The cost of the constituent materials (serving as an estimate of bulk quantities cost of the PCM) should be less than half of the projected storage system costs, or less than $50/kWh of storage capacity. The PCM weight and volume should also be "reasonable" for application to the back of a dish structure without substantially increasing dish structure costs (target under 3 tons (2700kg) and $1m^3$). Finally, the PCM must be able to be contained by cost-effective materials for long periods at high temperatures and many thermal cycles. The containment materials are also exposed to sodium (heat pipe) and air at the operating temperatures.

Our approach in this work is to identify potential PCM's through literature review and database-driven analytical studies [5] then verified by computational and experimental evaluation of the material thermal properties and compatibility.

2. PCM identification and selection

Over 40 potential heat transfer fluids and PCM's were identified in literature, including metallic elements, metallic eutectics, and salt eutectics [1]. While some of the more common PCM's were experimentally verified in the literature, the materials properties information was somewhat limited on many of the options. The list of potential options was reduced by downselecting metallic eutectics having a melting point near the target range of 750-800°C. In addition to the literature-identified options, we used thermodynamic modeling to identify potential calcium-based eutectic options for further study. The downselected list is shown in Table 1. The heat of melting was generally as predicted by FactSage [5]. From the heat of melting and the density, we are able to determine a mass and volume of PCM required for six hours storage. Using current commodity price estimates of the constituent materials, we can further bound the cost of the PCM required for six hours of storage (low end bound).

In Table 1 we can see that only four of the candidate materials meet the $\$50/kWh_{th}$ cost threshold. The MgSiZn eutectic was identified in literature [6] but the melt point and existence of a eutectic could not be confirmed in FactSage, the ASM tables, or through experimental synthesis. From this table, it should be noted that while CaSi has a very favorable price point, the mass is twice that of the CuMgSi ternary, and the volume a factor of four larger, meaning the cost for containment and heat transfer will be substantially higher. Therefore, we selected the CuMgSi ternary as the primary candidate, with CaSi as a backup alternative. Birchenall et. al [7, 8] previously identified the CuMgSi ternary as a leading candidate for CSP storage, and synthesized laboratory quantities after three attempts. Table 1 lists the candidates in priority order. CuSi is listed as a surrogate for the ternary while the feasibility of its synthesis was explored.

Table 1. PCM candidates selected based on melting point.

System			Weight Percent			Source	T_m [°C]	Cp_s [J/g.K]	Cp_s (T_m-1°C) [J/g.K]	Cp_L [J/g.K]	Cp_L (T_m+1°C) [J/g.K]	ΔH_m [J/g]	ρ_s(Tm-1°C) [g/cm³]	ρ_L(Tm+1°C) [g/cm³]	Mass for 400kWh (kg)	Volume 400kWh (m³)	Weight (lbm)	Cost ($)	Cost per kWh ($/kWh)
A	B	C	A	B	C														
Cu	Mg	Si	56	17	27	[5, 7]	742	0.540+(4E-04))T	0.853	0.9		548	5.06	3.2	2628	0.82	5793	14630	36.57
Ca	Si		97.25	2.75		[5]	785	0.482+(7E-04)T	1.033	0.875		180	1.55	1.4	8000	5.71	17637	7502	18.75
Cu	Si		82.97	17.03		[5, 7]	802	0.549+(8E-05)T	0.614	0.462+(E-04)T	0.542	267	-	6.09	5393	0.89	11890	37589	93.97
Ca	Bi		69	31		[5]	784					163.71†			8796		19392	21940	54.85
Al	Cu	Si	2.35	82.55	15.1	[5]	763	0.514+(9E-05)T	0.58	0.474+(E-04)T	0.55	258	-	6.07	5581	0.92	12305	38765	96.91
Mg	Si	Zn	48.25	37.84	13.91	[6]	FactSage does not show any ternary eutectic for this system					314	-	-	4586		10110	11949	29.87

† Heat of Melting estimated from elemental ratios

Initial efforts to synthesize the CuMgSi ternary were met with difficulties. The melting point differences between the constituents (650°C Magnesium through 1414°C Silicon) led to high magnesium vapor pressures prior to the melting of silicon. In addition, the literature varied greatly on the composition and melting point of the target eutectic (Table 2). We modified our approach and successfully made each of the compositions in the table. The approach consists of producing a CuSi mixture through arc melt techniques, and then adding stoichiometric amounts

of magnesium in a sealed ampule at under 1000 °C. The resulting products were then evaluated through Differential Scanning Calorimetry (DSC) to determine melt point and search for evidence of a eutectic mixture.

Three samples of CuMgSi were synthesized and are listed in Table 2 as FactSage, ASM diagram, and Birchenall, based on the source of the Wt. % of elements used. Both ASM and Birchenall samples showed some non-uniformity in appearance (Figure 2). Each has a darker appearance over about 1/3 of the slug, though the ASM discoloration is darker. In addition, the ASM sample had the primary slug and a second darker slug with a smooth finish. The slugs were broken apart, revealing that the darker areas were limited to surface discoloration (Figure 2). Micro XRF (X-ray fluorescence), a semi-quantitative tool, was used to verify the samples composition. Some contamination by W, Fe, and Al was evident in some XRF scans, but was not prevalent throughout the sample.

Table 2 CuMgSi eutectic formulations reported in the literature

	Wt%				At%				MP °C	Heat of Melting
	Cu	Mg	Si		Cu	Mg	Si			J/g
FactSage [5]	50.27%	24.51%	25.22%		29.33%	37.38%	33.29%		741	548
ASM diagram [9]	53.50%	21.16%	25.34%		32.20%	33.30%	34.51%		767	
Birchenall [7]	56.00%	17.00%	27.00%		34.67%	27.52%	37.82%		770	422.9

The FactSage composition synthesized by our team was also verified through digestion in HNO_3 and elemental analysis. This results in an unstable Si compound, which must be measured quickly to obtain closure in the results. On the final digestion, good closure was reached, with 1% unaccounted for: (49.7, 25.0, 24.0 wt % Cu-Mg-Si). This agrees well with the goal composition of this sample at (50.27, 24.51, 25.22 wt% Cu-Mg-Si), and the missing 1% is likely attributed to the unstable Si.

The thermal properties, primarily the melt point (or range) and the heat of melting, was determined with Differential Scanning Calorimetry (DSC) for each sample, following a sensitivity calibration against standards. Each sample was cycled four times within the DSC to verify consistent behavior with melt cycles (stability of the PCM).

Figure 2. ASM (left), Birchenall (second), FactSage (third) compositions of CuMgSi, including bottom portion of crucible. Broken piece of ASM sample (right) shows the dark discoloration was limited to the surface

For the ternary CuMgSi, DSC traces of both the FactSage (50% Cu, Figure 3) and Birchenall (56% Cu, Figure 5) compositions showed a slight double-peak during melting, indicating off-eutectic compositions. The Birchenall composition also showed a slight melting point change on subsequent cycles. In comparison, the ASM sample (53.5% Cu) showed excellent repeatability cycle-to-cycle (Figure 7), and a single peak indicating that it is a eutectic. The melt point of the ASM sample is determined to be 755°C (Figure 8).

The ASM sample also showed the highest heat of melting, 460 J/g, which is slightly higher than that reported by Birchenall [7] but lower than that predicted by FactSage [5]. The ASM phase diagrams do not report a heat of melting for this composition. The Birchenall composition sample showed a lower heat of melting at 406 J/g (

Figure **6**), while the FactSage composition sample (Figure 4), shows a heat of melting only 369 J/g, with an onset of melting at 753°C. Based on these results, it appears the ASM composition is a eutectic as evidenced by the highest heat of melting and the lack of double peaks. The measured heat of melting is suitable for further pursuit.

The CaSi composition was also tested by DSC in a covered crucible with high purity argon as the cover gas. This PCM, on several attempts, showed significant weight loss after melting the first time, and accurate heat of melting could not be obtained (Figure 9). We are trying to determine the cause of the weight loss, as analytical equilibrium analysis does not indicate a formation of a highly volatile composition, even when considering potential reactions with the crucible. We plan to re-test this sample in a sealed tantalum crucible. However, the DSC was contaminated by this test, and will be refurbished by the supplier before additional tests are attempted.

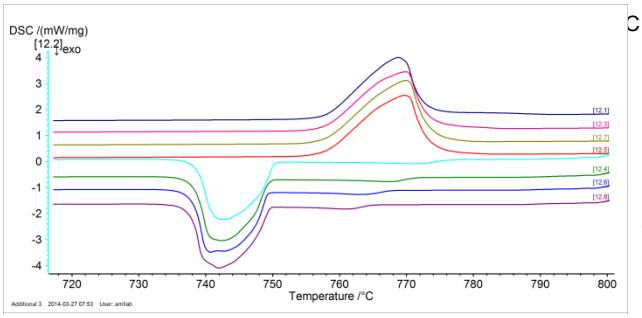

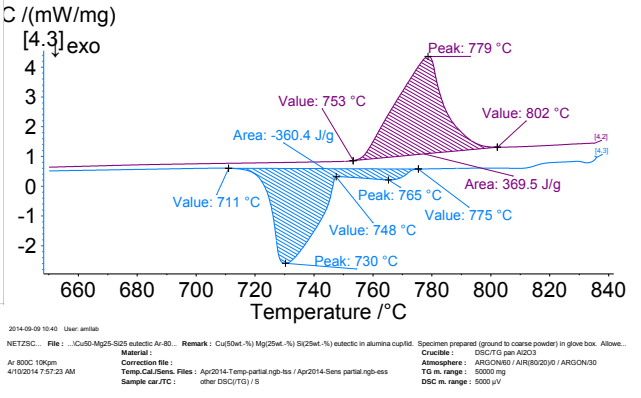

Figure 3. FactSage CuMgSi composition during 4 melt cycles in the DSC.

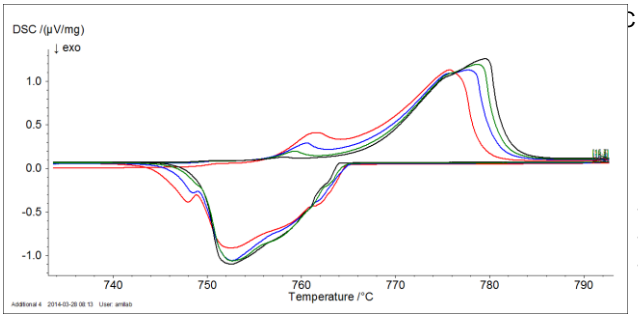

Figure 5. Birchenall CuMgSi composition during 4 melt cycles in the DSC, showing a slight second peak and shift in melt peak.

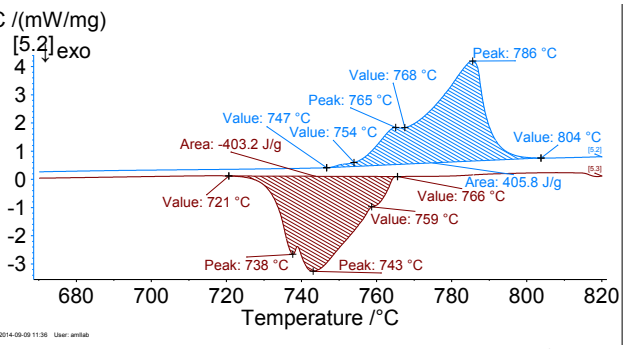

Figure 6. Birchenall CuMgSi composition showing the onset of melting (747°C) and the heat of melting (406 J/g).

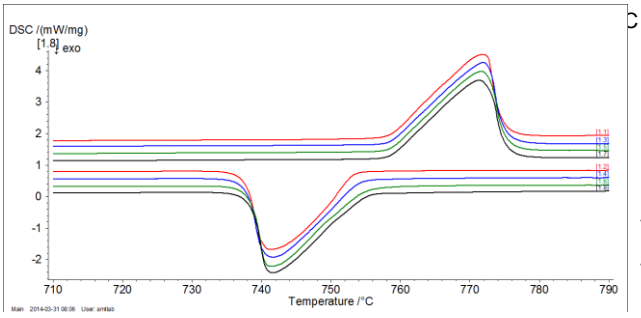

Figure 7. ASM CuMgSi composition during 4 melt cycles in the DSC, showing excellent repeatability and a single peak.

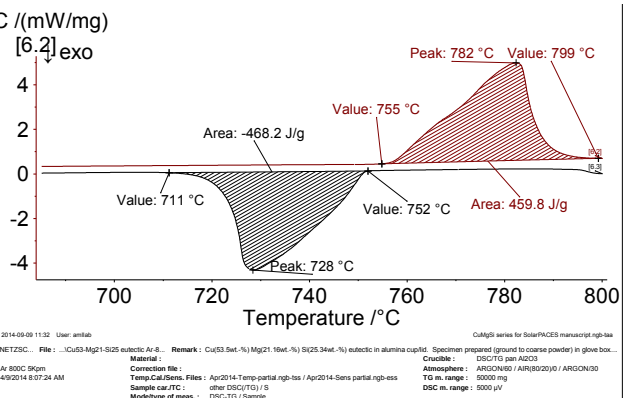

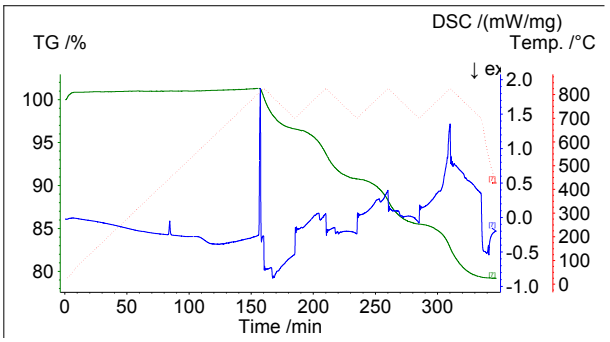

Figure 9. DSC cyclic characterization of the CaSi PCM, showing significant mass loss after the initial melt.

3. PCM containment compatibility

3.1. Containment options

Based on prior experience with liquid metal heat pipes, several conventional high performance alloys were identified for the containment material. Due to the aggressive corrosion possibilities of sodium (in the heat pipe), we desired to use alloys already proven compatible with sodium, and with reasonable strength at 800°C. Therefore, we explored 316L Stainless Steel, Inconel 625 nickel-based alloy (In625), and Haynes 230 nickel alloy (H230) with tungsten. The 316L is the lowest cost option of this set, but suffers from relatively fast oxidation at the proposed operating temperatures. However, due to its relative common use, it is possible that oxidation-resistant coatings may exist. The H230 has grown in popularity in CSP systems since it's first application to heat pipe receivers in at Sandia in the late 1980's [10]. This alloy is highly corrosion resistant and maintains good creep strength at 800°C. However, H230 is rather expensive. In625 is proposed as a mid-grade alternative, with more reasonable cost but less strength compared to the H230 alloy, and proven compatibility with sodium.

3.2. Thermochemistry modelling of PCM's and typical containment materials

We used commercial database-driven thermochemistry modeling packages to explore the potential for formation of compounds between the PCM alloy and the proposed containment alloy compositions. Chemical stability modeling of the PCMs was performed using the thermodynamics software HSC [11] to predict the potential for stable intermetallics that may form. This effort identified stable phases and their composition as a function of temperature after exposing FeNiCr (common constituents in the containment alloys) to Ca-Si and Cu-Si-Mg systems. Si and Mg-Ni intermetallics are shown to be stable at high temperatures. Evaluating the relative thermodynamic stability of Si intermetallics with Ellingham diagrams, the most stable compound was Ni_2Si followed by Cr_5Si_3 and Fe_3Si.

Stable intermetallic phases obtained from HSC are then assessed using phase diagram information from FactSage and include Fe-Si, Ni-Si, Cr-Si, Ni-Cr-Si, and Fe-Cr-Si. From these calculations intermetallics were predicted with melting points as low as 1000°C, close enough to our proposed operating point as to raise concern.

The intermetallic formation after exposing a Si containing liquid alloy with a substrate is of concern due to the high thermodynamic feasibility of degradation pathways through chemical interactions. While these results show the thermodynamic stability of many phases there is no indication of the kinetics at which reactions occur. Therefore, kinetics must be experimentally evaluated to determine if these compounds could exist in a metastable form or require a significant amount of time to be formed.

Peer review by the scientific conference committee of SolarPACES 2014 under responsibility of PSE AG.

3.3. Compatibility screening tests

Based on the thermodynamic calculations, we determined that short-term testing for acute interactions was prudent. These tests will likely form a basis for a suitable design for long-term compatibility testing. No literature data is available to provide expected kinetic rates at high temperatures of the interactions between the proposed PCM's and the shell materials. In order to maximize the possibility of success, all three proposed containment alloys were tested. Due to early difficulties in creating the ternary alloy only the binary Cu-Si alloy was tested at this point.

Tube stock (1/2" O.D.) was used for compatibility screening experiments. The tubes were bent into a "J" shape (Figure 10), had an end cap welded on the lower end, with a mini-conflat flange at the top end. The tailored shape of the tube ensured that PCM in liquid form would remain solely in the curved section, which is always the lowest physical location in the system. This eliminated the welds from short-term consideration. Once fabrication was complete the tubes were evacuated and baked out at 950°C to remove moisture and oxidation. A small quantity (5g) of the binary CuSi PCM alloy was added under an inert atmosphere glove box as solid pieces, and the tubes were sealed with Conflat flanges, providing a sealed inert Argon atmosphere. The tubes were then placed in a clamshell furnace, with the flanges kept outside to ensure seal temperatures below 200°C, as evidenced by the little oxidation observed in Figure 10 near the flanging. Exposures were 827.5±2.5°C for approximately 158 hours, ensuring the PCM was fully melted. After heating, the capsules were cross-sectioned and evaluated with X-ray Diffraction (XRD), Scanning Electron Microscopy (SEM)and Energy Dispersive Spectroscopy (EDS) area analysis to determine the presence and composition of new alloys. In addition, physical measurements were made on the exposed and unexposed polished cross sections to determine depth of affected zone.

All three containment alloys showed severe intermetallic diffusion of the PCM, resulting in significant wall loss. 29-30% wall loss was observed in all alloys despite the significantly different elemental compositions between the alloys. No mechanical wall failures were observed, though the rate of attack would likely lead to such failure in time scales orders of magnitude shorter than required for application to dish Stirling systems.

Figure 10. In625 configuration for materials screening tests. PCM is located in curved portion of the tube.

Nickel balanced alloys (HA230, In625) were found to have both copper and silicon diffusion layers impacting the base alloy (Figure 11). EDS area analysis determined that, within the diffusion layer, silicon had a relative weight percent greater than 25%, while copper was less than 6%. Outside of this silicon-rich diffusion zone there is a transition region, where ~65wt% is PCM constituents. It should be noted in HA230 that tungsten (W) did not scale linearly with the other alloying constituents. X-ray maps of W, Figure 11, indicate that this element appeared to be less mobile than other elements.

EDS of the PCM materials in regions appreciably further from the diffusion zones indicate the presence of nickel. It is clear that nickel is soluble to some extent as it is doubtful that solid-diffusion would result in a relative homogenous mixture through the melt. This behavior was not observed for the Fe balance alloy 316L.

316L exhibited no penetration of copper into the base alloy, nor in the obvious diffusion region. Silicon appeared to diffuse and alloy with the major elemental constituents of 316L (Fe, Cr, Ni) (see Figure 12). ASM phase diagrams indicate this theory is reasonable, shown in Figure 13, given the large number of phases possible for Fe-Cr-Si systems at 900°C.

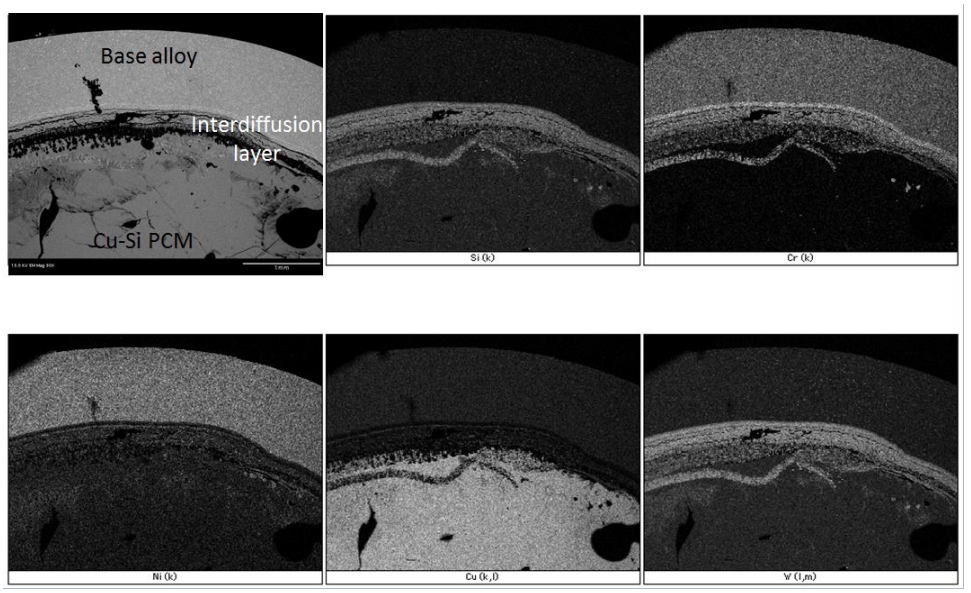

Figure 11: HA230 X-ray map indicating different intermetallic layers. Tungsten enrichment was observed due to the depletion of chromium and nickel from the base alloy.

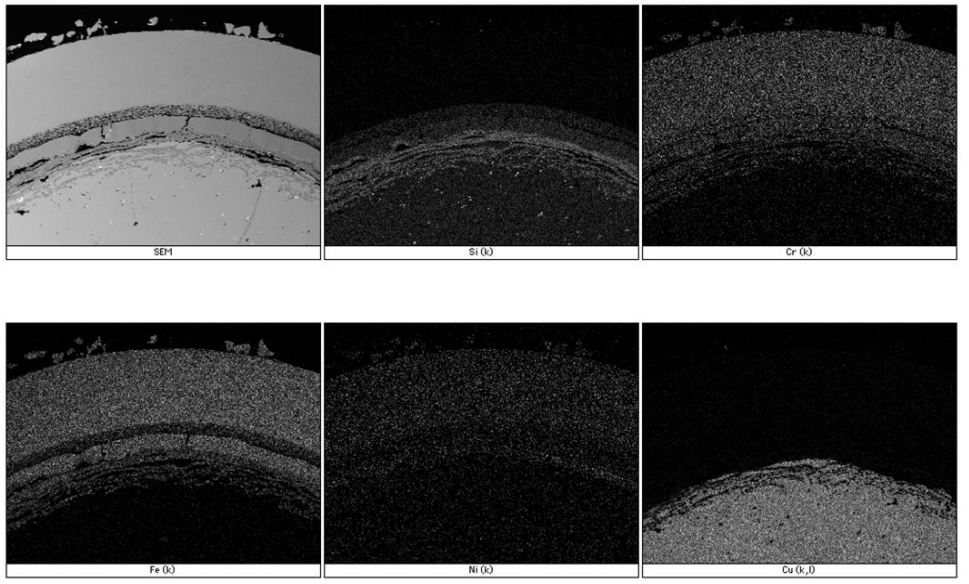

Figure 12: X-ray map 316L show no copper diffusion into the alloy, only silicon diffusion.

High magnification (SEM) analysis of the diffusion region, Figure 14, indicates that Si diffused into the innermost layer in contact with the base alloy. Spallation of the Fe-SI-Cr alloy appears near the surface, which may be the mechanism causing the high rate of material degradation. Upon inspection of the PCM, no obvious change from the original binary composition (Cu-17wt%Si) was observed. This observation is fundamentally different from the nickel based alloys, which had nearly 13-15% nickel present in the PCM.

3.4. Discussion of compatibility screening results

The short term testing clearly indicates that the proposed PCM will have compatibility issues with the considered containment materials. This leads to three possible solutions:

1. Consider alternative containment materials
2. Consider alternative PCM's
3. Consider protective coating options for the containment

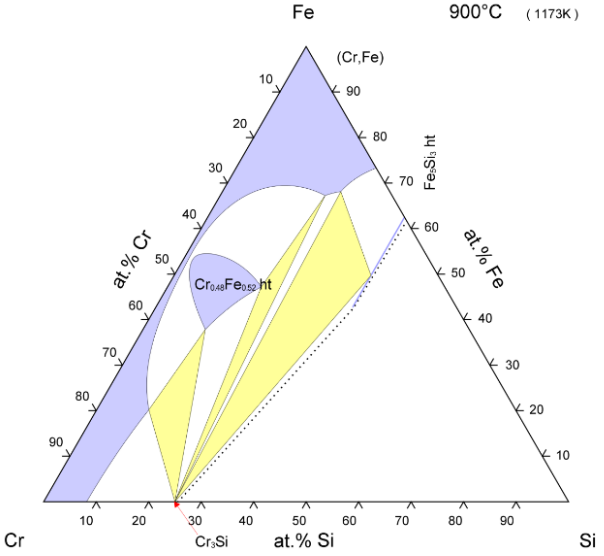

Figure 13: Ternary diagram for Fe-Cr-Si systems, indicating complex behavior at 900°C [12]. This diagram provides insight into the thermodynamic behavior over the duration of the test, however no kinetic information was available prior to high temperature tests.

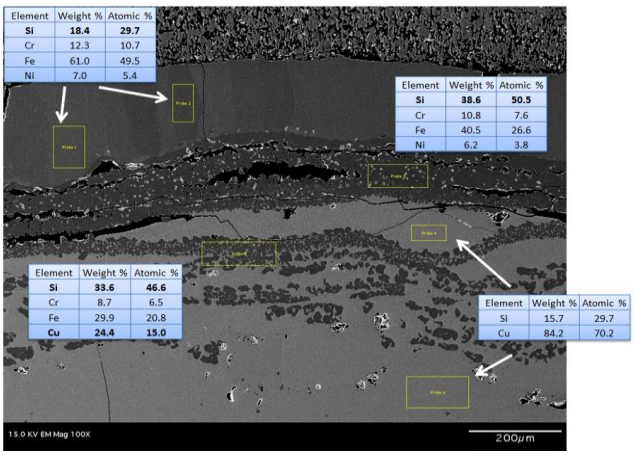

Figure 14: SEM image and EDS area analysis (indicated by yellow boxes) of 316L indicate in further detail no diffusion of copper was observed. Silicon was responsible for the intermetallic formation, which resulted in apparent spallation into the PCM. No soluble elements were present in the PCM.

Since the containment materials must also be compatible with sodium and air, and considerable work was performed in this area in the 1980's and 1990's, the first option is considered infeasible for a limited-budget project. The PCM search was extensive, considering both literature experience as well as exploring previously un-identified options. It appears that most, if not all, PCM's in the desired melt range will include silicon, which appears to be the primary negative actor. Therefore, it is unlikely that a suitable, compatible PCM will be located. A protective coating may be feasible, but must consider the following:

1. 100% coverage on a complex internal geometry of the storage unit. Therefore, line-of-sight coating processes may not be suitable, and priority must be given to approaches such as plating, vapor, and solution coating.
2. The coating must have robust adherence to the containment surface. The freeze-thaw cycle of the PCM may impose large shearing forces on the surface coating.
3. The coating must be compatible with both the containment substrate and the PCM. Long-term compatibility will have to be determined through testing
4. The coating must be flexible or have a reasonable CTE match to the substrate to avoid spalling during thermal cycling.

5. The coating must be relatively low cost so as not to drive the cost of the storage system

We have begun a coating development process in which we will analytically and experimentally determine potential coatings without acute compatibility issues, develop applicable coating application methods, and perform long-term exposure testing of the coatings on the selected substrate materials. The long-term testing will evaluate coatings on two time scales: 500 hours for application to a dish storage prototype, and 20,000 with no damage or evidence of passivation, for application to commercial implementations.

4. Conclusions

We have identified, successfully synthesized, and characterized a metallic-based PCM (CaSi and CuMgSi) for dish Stirling storage systems. The CuMgSi PCM has a very high heat of melting, minimizing the volume and mass of a 6-hour storage system, and presents a reasonable cost that can lead to a cost-effective storage system. While early literature reports varied, we were able to successfully make a near-eutectic alloy. During manufacturing studies, we used a more readily manufactured surrogate of CuSi for compatibility testing. Our findings for the PCM generally agree with late 1970's work at NASA [7, 8], though the final composition differs slightly.

We have demonstrated that acute compatibility issues exist between the selected PCM and proposed containment materials. The compatibility issues center on silicon, a component of most PCM's with appropriate melt temperatures. In addition, copper can present compatibility issues with some substrates. We propose to resolve these issues through a protective coating on the containment material, rather than developing or testing alternative containment materials ore PCM's.

Success in the selection and development of a PCM and containment system may lead to cost effective thermal storage for dish Stirling systems. This storage, centering on a phase change material, would provide an excellent match to the isothermal input feature of Stirling engines, and would expand the applicability of high performance dish Stirling systems for CSP production.

Acknowledgements

Sandia National Laboratories is a multi-program laboratory managed and operated by Sandia Corporation, a wholly owned subsidiary of Lockheed Martin Corporation, for the U.S. Department of Energy's National Nuclear Security Administration under contract DE-AC04-94AL85000.

References

[1] Andraka, C. E., 2012, "Technical Feasibility of Storage on Large Dish Stirling Systems," No. SAND2012-8352, Sandia National Laboratories, Albuquerque NM.

[2] Andraka, C. E., 2013, "Dish Stirling Advanced Latent Storage Feasibility," Elsevier Energy Procedia, 49, pp. 684-693.

[3] Andraka, C. E., 2011, "High Performance Thermal Storage Solutions for Dish Stirling Systems," No. 0471-1578, ARPA-E HEATS FOA proposal.

[4] Shabgard, H., Faghri, A., Bergman, T. L., and Andraka, C. E., 2013, "Numerical Simulation of Heat Pipe-Assisted Latent Heat Thermal Energy Storage Unit for Dish-Stirling Systems," ASME 2013 International Mechanical Engineering Congress & Exposition, ASME, San Diego, California.

[5] CRCT-Thermfact Inc., and GTT-Technologies, 2010, "FactSage," ver. 6.3, http://www.factsage.com/.

[6] Farkas, D., and Birchenall, C. E., 1985, "New eutectic alloys and their heats of transformation," Metall and Mat Trans A, 16(3), pp. 323-328.

[7] Birchenall, C. E., Guceri, S. I., Farkas, D., Labdon, M. B., Nagaswami, N., and Pregger, B., 1981, "Heat Storage in Alloy Transformations," No. DOE/NASA/3184-2, NASA CR-165355, University of Delaware.

[8] Birchenall, C. E., and Riechman, A., 1980, "Heat storage in eutectic alloys," Metall and Mat Trans A, 11(8), pp. 1415-1420.

[9] ASM International, 2012, "Alloy Phase Diagram Center," http://www1.asminternational.org/asmenterprise/apd/.

[10] Andraka, C. E., Moreno, J. B., Diver, R. B., and Moss, T. A., 1992, "Sodium Reflux Pool-Boiler Solar Receiver On-Sun Test Results," No. SAND89-2773, Sandia National Laboratories, Albuquerque NM.

[11] Outotec, 2011, "HSC Chemistry Software," ver. 7.11, http://www.outotec.com/en/Products--services/HSC-Chemistry/.

[12] Chart, T., 1980, "Cr-Fe-Si Phase Diagram," Alloy Phase Diagram Database, ASM International, Materials Park, OH, 2006, http://www1.asminternational.org/AsmEnterprise/APD.